7

Assembly and Characterization of Biomolecule–Gold Nanoparticle Conjugates and Their Use in Intracellular Imaging

Alexander Tkachenko, Huan Xie, Stefan Franzen, and Daniel L. Feldheim

Summary

In this chapter, we outline protocols for assembling and characterizing peptide–gold nanoparticle conjugates. We describe two strategies for attaching peptides to gold nanoparticles. One involves the covalent coupling of cysteine-terminated peptides directly to a particle surface via a sulfur-gold bond. Alternatively, peptides are coupled to bovine serum albumin (BSA) via a bifunctional molecular crosslinker. We also describe a number of characterization methods for determining the number of crosslinkers per BSA, peptides per BSA, and peptides adsorbed per particle. Finally, we show that the enormous visible light extinction properties of gold nanoparticles make them excellent imaging agents for tracking the trajectories of peptides inside living cells.

Key Words

Gold nanoparticles; cell imaging; bovine serum albumin; polyethylene glycol; peptides; microscopy.

1. Introduction

Protocols for assembling peptide–gold particle conjugates and monitoring their trajectories inside cells are detailed in this chapter. Gold particle bioconjugates are important constructs for cellular imaging, therapeutic delivery, and biomolecule detection ***(1–3)***. Because of the remarkably large scattering cross-section of metal particles (10^{-10} cm^2), individual nanoparticles can be imaged under white-light illumination. Moreover, the plasmon resonance condition of metals can be tuned across the visible spectrum and into the near infrared simply by changing particle size and shape ***(4,5)***. Thus, multicolor assays are

From: *Methods in Molecular Biology, vol. 303: NanoBiotechnology Protocols*
Edited by: S. J. Rosenthal and D. W. Wright © Humana Press Inc., Totowa, NJ

possible with a single light source, without the need for filters, and free from complications of fluorescence bleaching or blinking.

A potential application of gold particle bioconjugates is therapeutic delivery. A primary goal of modern therapeutic delivery is to create a bioconjugate capable of seeking out specific cells in vivo, traversing the cell and nuclear membranes, and releasing a therapeutic in the nucleus. Recognizing the multitude of challenges associated with nuclear targeting, and following the presumption that no single peptide will be effective at *specific* cell recognition and nuclear targeting, we have been pursuing a new approach to nuclear translocation. The general strategy has been to combine multiple membrane translocating peptides and antibodies on a *single* gold nanoparticle scaffold. Of paramount importance in the construction of multipeptide nanoparticles is understanding how to formulate peptide-gold bioconjugates that are stable in high ionic strength solutions containing exchangeable peptides and proteins found in cellular media, and how to quantitate the number of adsorbed biomolecules per gold particle (*see* **Note 1**). Protocols for performing these studies are described herein. These experiments are then followed by a description of methods for imaging gold nanoparticles inside cells using video-enhanced color differential interference contrast (VECDIC) microscopy.

2. Materials

1. Hydrogen tetrachloroaurate.
2. Sodium citrate.
3. Bovine serum albumin (BSA) (highest purity) (Roche, Indianapolis, IN).
4. 3-Maleimido benzoic acid *N*-hydroxysuccinimide (MBS) (Pierce, Rockford, IL).
5. Gold nanoparticles (20-nm diameter) (Ted Pella).
6. Dimethylformamide (DMF).
7. 50 m*M* phosphate buffer, pH 7.0, with 50 m*M* EDTA.
8. EDTA.
9. Dithiothreitol (DTT).
10. Fluorescamine (4-phenyl-spiro [furan-2(3H), 1′-phthalan]-3,3′-dione).
11. Rhodamine B isothiocyanate (RBITC).
12. Cysteine-terminated peptides.
13. Lysine.
14. Thiolated methoxy polyethylene glycol (PEG), 5000.
15. Acetone.
16. Membrane filter (0.8 μm).
17. Sephadex G-50 (Sigma, St. Louis, MO).
18. Chromatography equipment.
19. Centricon YM-30 and Microcon YM-100 (Millipore, Bedford, MA).
20. Sodium dodecyl sulfate polyacrylamide gel electrophoresis (SDS-PAGE) equipment.
21. Microplate absorbance and fluorescence reader.

22. Optical research microscope equipped with differential interference contrast (DIC) optic.
23. Scientific-grade color digital camera (at least 1 million pixels).

3. Methods

3.1. Synthesis of Gold Nanoparticles

Gold nanoparticles are synthesized in a one-step aqueous preparation in which hydrogen tetrachloroaurate is brought to boiling and reduced by rapidly adding sodium citrate ***(6)***. Particle diameter can be tuned via citrate : $[AuCl_4]^{1-}$ stoichiometry. The resulting particles are ready immediately for conjugation to peptides or proteins.

1. In a 1-L round-bottomed flask equipped with a condenser, heat 500 mL of 1 m*M* $HAuCl_4$ solution to boiling point with vigorous stirring.
2. After refluxing for 10 min, rapidly add 50 mL of 40 m*M* of trisodium citrate to the stirring solution. The color should change from a pale yellow to a deep wine red.
3. Let the solution boil for 10 min.
4. Remove from the heat and continue to boil for an additional 15 min.
5. Remove the stir bar and allow the solution to cool to room temperature.
6. Filter through an 0.8-µm membrane filter.
7. Characterize using visible spectroscopy and transmission electron microscopy (TEM). This prep yields about 12-nm-diameter particles with peak absorption at 520 nm.

3.2. Assembly of Biomolecule–Gold Nanoparticle Complexes

Two strategies for attaching cell-targeting peptides to gold nanoparticles are described (**Fig. 1**). One involves the covalent coupling of cysteine-terminated peptides directly to a particle surface via a sulfur-gold bond. Alternatively, peptides are coupled first to BSA via the bifunctional crosslinker MBS and then attached to gold nanoparticles via electrostatic interactions ***(7)***. There are advantages and disadvantages for each strategy. The direct coupling of cysteine-terminated peptides to gold particles affords a simple one-step procedure that produces particles with a high surface coverage of peptide. However, many peptides are sparingly soluble in aqueous solution or cause flocculation when attached to gold nanoparticles. Attaching peptides to BSA prior to immobilization on gold nanoparticles creates extra chemical reaction and purification steps but can increase peptide solubility and sol stability.

3.2.1. Conjugation of Peptides to BSA

Peptides are conjugated in two steps. In step 1, lysine residues of BSA are treated with the heterobifunctional crosslinker MBS. The maleimide moieties of

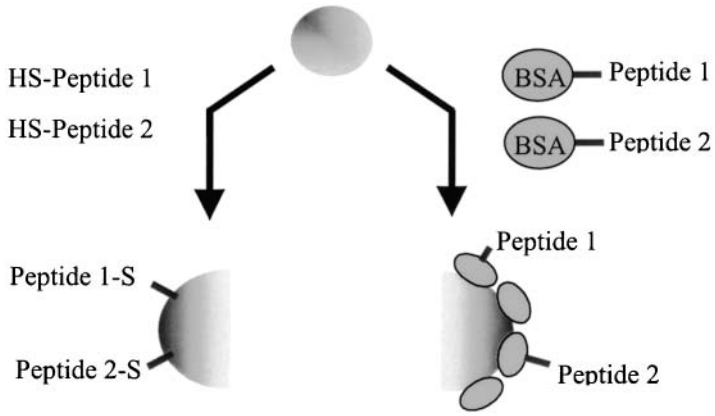

Fig. 1. Two strategies for assembling multifunctional gold particle–peptide bioconjugates.

the BSA-MBS complex react with free thiols of the peptide terminal cysteine residue. Right side of the diagram illustrates use of a protein linker, while left side shows covalent attachment via a thiol-gold bond.

1. Prepare an aqueous solution of high-purity BSA (5–10 mg/mL) in degassed 50 m*M* phosphate buffer, pH 7.0, with 50 m*M* EDTA.
2. Dissolve MBS in DMF (10 mg/mL).
3. Within 30 min add the solution of MBS to aqueous solutions containing BSA in molar ratios of the linker to BSA of between 1:2 and 1:100. (BSA contains 59 lysine residues, of which up to 35 can be used for MBS modification ***[8]***).
4. Allow the reaction to proceed for 60 min at room temperature.
5. Remove the unreacted MBS linker by gel filtration using Sephadex G-50 or by centrifugal solvent displacement (Centricon YM-30 at 5000*g*). (Maleimides can undergo hydrolysis; therefore, thiol binding should be performed within hours of purifying excess MBS from the BSA-MBS complex).
6. Dissolve 5 mg of lyophilized peptide containing terminal cysteine in degassed 50 m*M* phosphate buffer, pH 7.0, with 50 m*M* EDTA.
7. Because the sulfhydryl groups in the peptide may oxidize, it is often necessary to pretreat the peptide with a reducing reagent such as DTT prior to coupling with BSA-MBS. Mix 5 mg of peptide with 5 mg of DTT and let it react for 1 h at room temperature.
8. Separate the peptide from free DTT using an equilibrated Sephadex G10 column with 1% acetic acid. The first fraction will contain the peptide and the second fraction will contain free DTT.
9. Mix BSA-MBS conjugates with peptide solution at the desired ratio (2–50:1 peptide:BSA) and react in pH 7.4 buffer for at least 3 h at 4°C.

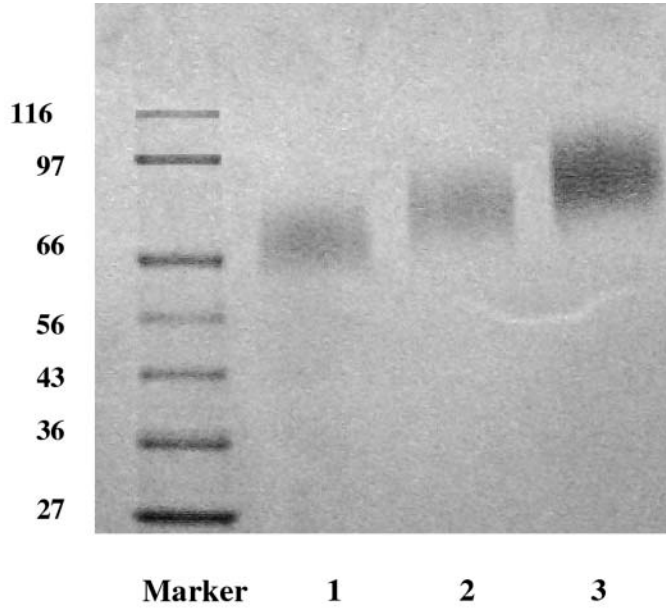

Fig. 2. Gel shift assay, 7.5%, SDS-PAGE gel: lane 1, BSA/MBS complex at 1:40 ratio; lane 2, BSA/peptide at 1:3 ± 1 ratio; lane 3, BSA/peptide at 1:6 ± 2 ratio. The broad nature of the sample bands reflects various binding efficiencies within the sample. Marker bands correspond to the molecular weight in thousands on the left.

10. Remove the unreacted peptides by dialysis or by centrifugal solvent displacement (Centricon YM-30 at 5000*g*).
11. Analyze the prepared BSA-peptide complexes using 7.5% polyacrylamide gel electrophoresis (SDS-PAGE). An example is shown in **Fig. 2**.

3.2.1.1. Characterization of BSA-MBS Complexes by Fluorescamine Assay

Because the purity of BSA varies and the binding efficiency of the *N*-hydroxysuccinimide (NHS) moiety of MBS is strongly affected by water and pH, it is important to investigate quantitatively the number of MBS ligands attached to BSA. This can be determined using a fluorescamine assay, which measures the number of unreacted lysine residues following MBS conjugation (*see* **Note 2**):

1. Dissolve fluorescamine in high-performance liquid chromatography–grade acetone (3 mg/mL) to obtain a 1 m*M* solution. (The use of acetone presents a set of unique problems, because commonly used polystyrene disposable pipets are incompatible. Glass or polypropylene materials, with their higher resistance to organic solvents should be used.)

2. Prepare appropriate lysine standards (0–500 μ*M*) and BSA-MBS (100–500 μg/mL) samples in 50 m*M*, pH 7.4 phosphate buffer.
3. Add a 250 μ*M* solution of fluorescamine to the prepared samples. (If plastic is used, the fluorescamine solution should be no more than 25% of the total reaction volume. For standard 96-well microplate assays, 50 μL of stock fluorescamine solution is added to 150 μL of sample.)
4. Mix thoroughly.
5. Read the fluorescence with a 390/30-nm excitation filter and a 460/40-nm emission filter. If samples remain sealed and protected from light, the reaction will be stable for 2 h.
6. Determine the number of bound MBS per BSA from the difference of total and unreacted lysines.

3.2.2. Attachment of Peptide-BSA Conjugates to Gold Nanoparticles

The following protocols for attaching peptide-BSA conjugates to gold nanoparticles will vary slightly depending on the particular choice of peptide. In general, to avoid particle flocculation, the pH of the peptide-BSA conjugate should be adjusted to a value close to the isoelectric point (p*I*) of the peptide prior to addition to the gold nanoparticle sol. The following example is for a peptide with a p*I* close to pH 9.0. Note that all glassware must be clean.

1. Add dropwise with rapid stirring 0.1 mL of 10 μ*M* freshly prepared peptide-BSA conjugate (in 10 m*M*, pH 9.0 carbonate buffer) to 0.9 mL of 20-nm-diameter citrate-passivated gold nanoparticles (1.16 n*M*) to achieve a ratio of approx 1000 protein molecules per gold nanoparticle ***(9)***.
2. Incubate the mixture on a shaker for 30 min.
3. Centrifuge the solution at 12,000*g* for 1 h at 4°C to separate the unbound peptide-BSA from the conjugates.
4. Carefully remove the supernatant containing unbound peptide-BSA and resuspend the pellet in carbonate buffer (10 m*M*, pH 9.0) to obtain peptide-BSA-coated gold nanoparticles.

3.2.3. Attachment of Peptides Directly to Gold Nanoparticles

Thiols form covalent bonds to metals such as gold and silver. Thiol-gold chemistry is being employed in a wide range of biomolecule-sensing strategies, including a gold particle colorimetric assay for DNA ***(10)***. One of the more appealing aspects of thiol-gold chemistry is that the reaction proceeds at room temperature in aqueous solution. Moreover, attaching many different functional thiols to a single particle is typically as simple as stirring all the ingredients together in one pot ***(11)***.

For a 20-nm colloid, the thiolated species are typically added so as to achieve a molar ratio of approx 2500 thiols per nanoparticle. To ensure monolayer coverage, this ratio can be adjusted according to the core size of the colloids; the

available number of adsorption sites is directly proportional to the total surface area and thus to the square of the particle diameter. If a mixed thiol monolayer is sought, the desired thiols may simply be stirred in solution together with gold particles and allowed to adsorb. In many cases, the mole fraction of thiols bound to nanoparticles will reflect the mole fraction added to the reaction mixture ***(11)***. Mixed monolayers of PEG and peptides are synthesized as follows. Note that all glassware must be clean.

1. Combine 72 μL of thiolated PEG (20 μ*M*) and 72 μL of peptide (20 μ*M*) to produce a molar ratio of PEG to peptide of 1 : 1.
2. Add 145 μL of this mixture to 1 mL of 20-nm-diameter citrate-capped gold nanoparticles (1.16 n*M*) to produce a molar ratio of thiol to gold of 2500 : 1.
3. Stir the mixture of gold/PEG/peptide at room temperature for 1 h to allow complete exchange of thiol with citrate on the gold nanoparticles.
4. To purify the complex, centrifuge at 12,000*g* for 30 min.
5. Decant the supernatant and resuspend the pellet in 1 mL of water.

3.3. Characterization of Peptide–Gold Nanoparticle Complexes

The number of peptide-BSA conjugates attached to gold can be determined by radiolabeling, fluorescence spectroscopy, and time-correlated single-photon counting spectroscopy (TCSPC) ***(12)***. TCSPC requires relatively sophisticated laser equipment and expertise but has the advantage of being able to probe the dynamics of protein or peptide adsorption and exchange on gold nanoparticles without separation steps. Here we focus on the more routine static fluorescence techniques used in our laboratory for characterizing protein–gold particle conjugates.

Peptide-BSA binding isotherm measurements on gold nanoparticles can be constructed as follows:

1. Label the protein (or attached peptide) with a fluorophore. In this example, BSA was modified with RBITC. Similar procotols may be used for fluorescently tagged peptides.
2. Prepare 9 × 30 μL solutions of RBITC-BSA in concentrations ranging from 0.4 to 12 μ*M* *i*n 10m*M* pH 7 phosphate buffer.
3. To each protein solution, add 450 μL of a 1.05 n*M* solution of gold nanoparticles and stir for 15 min. Native BSA may be added to each solution to increase stability against particle aggregation. Caution must be taken, however, that the exchange of the added native BSA for surface-bound protein does not occur during the course of the experiment. To improve the stability of RBITC-BSA–gold nanoparticle conjugates, 20 μL of 2 mg/mL native BSA (e.g., unlabeled BSA) was added to each solution ***(13,14)***.
4. Remove the unbound fraction of RBITC-BSA by centrifuging the solutions at 10,000*g* for 30 min. Collect the supernatant.

5. Repeat **step 4**.
6. Dilute all the supernatants to 2 mL by pH 7.0, 10 m*M* phosphate buffer. Measure the fluorescence intensity of each sample, and compare the fluorescence to a standard curve to determine the concentration of unbound RBITC-BSA in the initial mixture.
7. Calculate the amount of RBITC-BSA bound to the gold particles by subtracting free RBITC-BSA from the total amount of RBITC-BSA added initially.

An adsorption isotherm for BSA conjugates is shown in **Fig. 3**. Formally, adsorption isotherms are only valid for systems in equilibrium. Two experimental findings are suggestive of equilibrium adsorption in the systems studied here: (1) the amount of BSA adsorbed per particle did not change over the course of several hours; and (2) BSA desorbed, albeit slowly, over time. Nonlinear regression was applied to analyze the RBITC-BSA saturation curve. A one-site binding model yielded a K_d of 101.4 n*M* and a saturation coverage of 158 RBITC-BSA/gold nanoparticle ***(9)***.

This curve suggests a substantial amount of multilayer adsorption may occur for these BSA conjugates on gold nanoparticles. Thus, care must be taken to measure adsorption isotherms for each new peptide-BSA–gold nanoparticle construct.

3.4. Intracellular Imaging of Colloidal Gold With Light Microscopy

Silver and gold colloids have been of interest for thousands of years because of their unique visible optical properties. The efficiency for the extinction of light (absorption plus scattering) by metal nanoparticles surpasses by orders of magnitude that of any molecular chromophore. In addition, both absorption and scattering properties can be considerably altered by surface modification, or by electronic coupling between individual nanoparticles ***(1,15,16)***. Together with an exceptional resistance to photodegradation, such favorable optical features are making metal colloids attractive components for diagnostic, electronic, and photonic devices. Metal nanoparticles modified with many different cell-targeting agents and therapeutics could also be attractive components for therapeutic delivery ***(3,17)***.

TEM remains the best technique in terms of spatial resolution (~1 nm) for viewing colloidal nanoparticles in biological samples, but it requires laborious sample preparation and expensive equipment. Live cells, however, can only be imaged using light microscopy, and various techniques have been employed to enhance the visibility of colloidal gold particles, which are typically smaller than the resolution limit of light microscopy. With video-enhanced light microscopy, structures that are an order of magnitude smaller than the resolution limit of the light microscope can be detected ***(18,19)***. Individual gold particles of 20-nm diameter can be observed with reflection-contrast microscopy

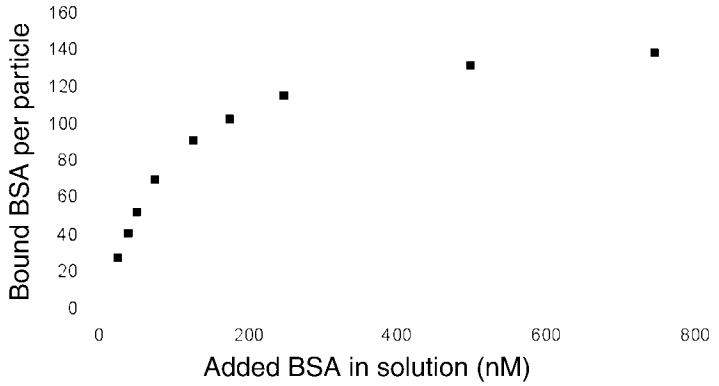

Fig. 3. Adsorption isotherm of RBITC-labeled BSA adsorbed on gold particles (20 nm in diameter).

(20,21) and high-contrast video microscopy (Nanovid) ***(22)***, and the use of video-enhanced light microscopy to image colloidal gold inside living cells has been reported ***(23–25)***.

Note, however, that there are several caveats to the optical imaging techniques just described. First, nanoparticles are only identified as an inflated diffraction image. Thus, a 20-nm-diameter particle will appear as an approx 200-nm particle in the optical image (the diffraction limit). Second, these techniques often require second-image and post-image processing to visualize cellular structures. Finally, some cellular structures such as out-of-focus dense granules may also appear in an enhanced image as bright or dark spots, and it is often difficult to distinguish these structures from nanoparticles unless polarization optics and color imaging are used ***(1,3)***.

3.4.1. VECDIC Microscopy

Introducing color into the imaging system capitalizes on the ability of nanoparticles to reflect polarized light at wavelengths different from that of the surrounding biological media; thus, silver and gold nanoparticles can be simultaneously observed inside living or fixed cells via single-pass VECDIC microscopy (**Fig. 4**).

3.4.1.1. Hardware Configuration of VECDIC Microscopy

VECDIC microscopy can be performed with any research-grade DIC-equipped microscope using Nomarski or de Sénarmont bias retardation. The light upright microscope Leica DMLB has been used routinely for these studies with a standard image-splitting prism, which can direct 0, 50, or 100% of

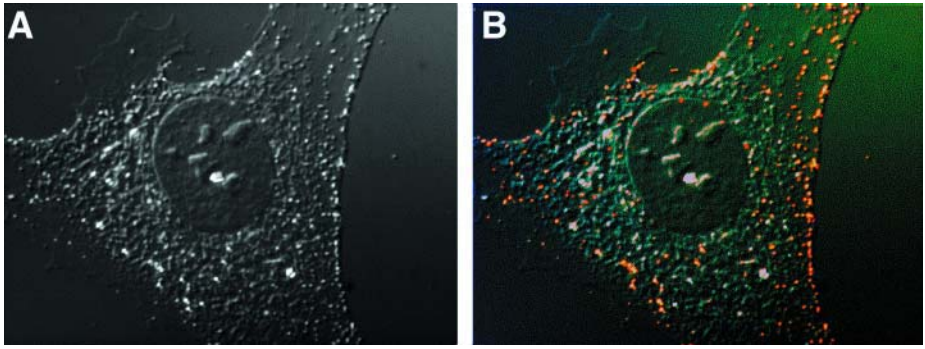

Fig. 4. Comparison of **(A)** video-enhanced black-and-white DIC microscopy and **(B)** video-enhanced color DIC microscopy. Shown are 20-nm-diameter gold-peptide-BSA complexes inside 3T3 cells. Images were taken with a Nikon DXM 1200 digital color CCD camera on a Leica DMLB DIC-equipped microscope with a ×100/1.3 NA objective.

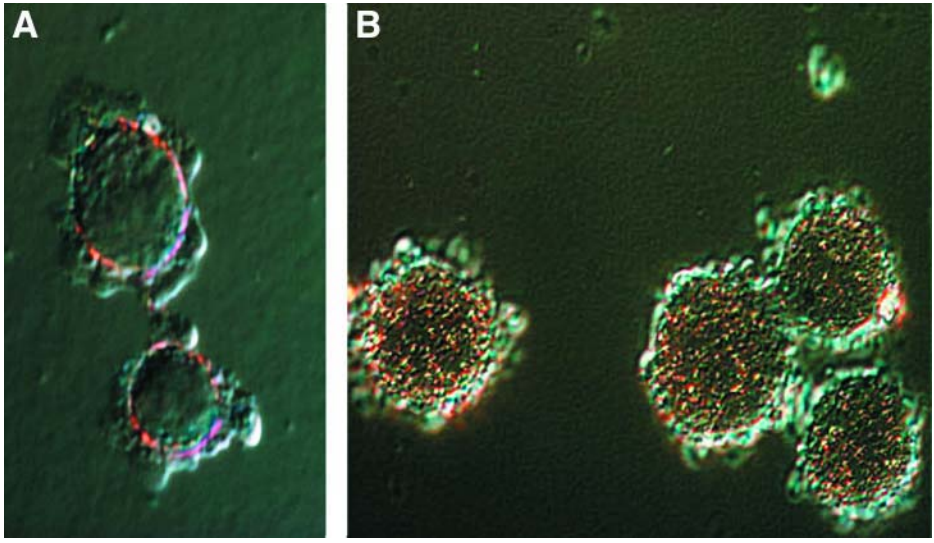

Fig. 5. Incubation of HeLa cells with 20-nm gold nanoparticles after 3 h by VECDIC microscopy. **(A)** Nanoparticle carrying Large T NLS accumulated around nuclear membrane. **(B)** Nanoparticle carrying adenovirus NLS accumulated inside nucleus.

the light into the camera. The microscope was equipped with a 0.9 numerical aperture (NA) condenser and Nomarski DIC optics. Illumination was supplied from a 100-W halogen light source. The strain-free Plan Apo ×63–100 objectives (NA 1.00–1.4) are suitable for this purpose. Oil immersion objectives

should be used to eliminate reflections from the surface-air interface of the microscopic slide. High NA oil condenser and light-scrambling techniques using fiberoptic illumination can dramatically improve resolution of VECDIC microscopy. Our video system comprises a Nikon DMX-1200 color charge-coupled device (CCD) digital camera, with software-based manual control of individual color channels and contrast enhancement on live and captured images. The ability to use video enhancement on live images is essential for video-enhanced microscopy. Manual control of the camera video enhancement setting is also necessary, because an automatic camera will continuously adjust brightness and contrast to accommodate bright spots inherent in DIC microscopy, which makes it difficult to compare acquired images.

3.4.1.2. Operation of VECDIC Microscope

A microscope should be equipped with DIC optics using Nomarski or de Senarmount bias retardation and color camera with video enhancement capabilities.

1. Adjust the microscope for Köhler illumination and switch to a high-magnification objective (×60–100).
2. Insert the polarizer and analyzer in the optical path of the microscope set up for bright field, and examine the objective rear focal plane with a phase telescope or Bertrand lens. If the polarizer and analyzer are properly positioned and the microscope perfectly aligned, a dark extinction cross will appear in the objective aperture. (This step may not be necessary if the optic was properly aligned before.)
3. With the microscope aligned for Kühler illumination and set up for DIC (the polarizer and analyzer crossed, and both prisms [objective and condenser] installed), place a sample on the stage and focus the specimen while observing the procedure through the eyepieces. In general, the specimen assumes a pseudo-three-dimensional appearance with a shadow-cast effect.
4. Rotate the objective DIC prism or rotate the polarizer (or analyzer) in the microscope equipped for de Sénarmont compensation to achieve maximum extinction. The image should appear very dark gray at maximum extinction. Gold nanoparticles >40 nm should be observed at this setting as bright yellow or red dots. Reducing the size of the condenser aperture diaphragm can significantly improve the observation of gold nanoparticles.
5. Switch the image from the viewfinder to the attached color video camera.
6. Using the video enhancement features of the camera, optimize the contrast and color setting for observation of yellow/red gold nanoparticles. Optimizing bias retardation and aperture diaphragm on the microscope will allow simultaneous observation of cellular structures and gold nanoparticles (*see* **Note 3**).

3.5. Intracellular Imaging of Peptide–Gold Nanoparticle Conjugates

The nucleus is the desired target for cancer therapies that involve DNA–drug-binding interactions, gene therapy and antisense strategies that manipulate RNA splicing. Although viruses have been adapted to deliver genes to cell nuclei, the design of safer synthetic delivery systems remains a challenge. The functionally active peptide sequences of nuclear localization signals (NLSs) of many viral proteins are known. Such peptides could be synthesized with a terminal cysteine residue and attached to a nanoparticle along with therapeutic agents. The following example demonstrates nuclear targeting of gold particles modified with NLS peptides derived from SV-40 and adenoviruses (**Fig. 5**).

1. Order the desired peptide with terminal cysteine.
2. Prepare a peptide-BSA conjugate (*see* **Subheading 3.2.1.**).
3. Attach the peptide-BSA conjugate to a 20-nm-diameter citrate-coated gold nanoparticle (*see* **Subheading 3.2.2.**).
4. Incubate the desired cell line (e.g., 3T3, HeLa) on 1.5 microscopy cover slips until they reach 60–70% confluency.
5. Add nanoparticles carrying NLS to the cell growth media.
6. Incubate the cells with the nanoparticles in growth media for 1–6 h.
7. Stop incubation at the specified time by removing the media.
8. Rinse the cells with DPBS five times to remove nanoparticles in the growth media.
9. Fix the cells in 4% paraformaldehyde for 15 min and replace with Dulbecco's phosphate buffered saline (DPBS).
10. Mount cover slips containing cells on a microscopy slide using Fluorosave mounting media.
11. Let the mounting media dry overnight.
12. Image the cells using VECDIC microscopy (*see* **Subheading 3.4.1.**).

4. Notes

1. The stability of colloidal sols is owing to a balance of forces including electrostatic repulsion, van der Waals attraction, and mixing free energy. The former two forces have been condensed into the well-known Derjaquin, Landau, Verway, Overbeck (DLVO) theory ***(26)***, which explains the stability of charged particles. The stability of colloidal sols is often improved with the use of "steric stabilizers." These are typically large proteins or polymers, placed in solution at concentrations often 1000 times the particle concentration. Proteins and polymers may adsorb to the particle surface strongly, in which case stabilization is afforded simply by the large positive free energy of desorption required prior to particle–particle fusion. Polymer chains that are free in solution, however, may also influence colloidal stability. Polymers in solution can cause particle flocculation or stabilization ***(26)***. Flocculation occurs whenever colloidal

particles approach so closely that the free polymer is excluded from the interparticle region. This is an entropic effect; the polymer leaves the interparticle region in response to the loss of configurational entropy on compression by the particles.

2. BSA has multiple lysine residues for reaction with the NHS moiety of MBS. The nonfluorescent compound fluorescamine (4-phenyl-spiro [furan-2(3H), 1′-phthalan]-3,3′-dione) reacts rapidly with primary amines in proteins, such as the terminal amino group of peptides and the ε-amino group of lysine, to form highly fluorescent pyrrolinone-type moieties *(27)*. The number of MBS ligands coupled to BSA can thus be determined with the fluorescamine assay by measuring the number of unreacted lysine residues following MBS conjugation.
3. When tracking the trajectories of nanoparticles inside cells, it is important to be able to distinguish the relative location of particles inside (or outside) the cell in both the x-y and z directions. Because the depth of field in DIC is very shallow, optical z sectioning is possible with VECDIC. Thus, it is usually possible to discriminate between nanoparticles inside or outside the cell or nucleus. It must be remembered that DIC is a pseudo-three-dimensional imaging technique. The size of objects in the z direction is thus the result of the optics and may not be representative of the actual feature size.

References

1. Schultz, S., Smith, D. R., Mock, J. J., and Schultz, D. A. (2000) Single-target molecule detection with nonbleaching multicolor optical immunolabels. *Proc. Natl. Acad. Sci. USA* **97,** 996–1001.
2. Feldherr, C. M., Lanford, R. E., and Akin, D. (1992) Signal-mediated nuclear transport in simian-virus 40-transformed cells is regulated by large tumor-antigen. *Proc. Natl. Acad. Sci. USA* **89,** 11,002–11,005.
3. Tkachenko, A. G., Xie, H., Coleman, D., Glomm, W., Ryan, J., Anderson, M. F., Franzen, S., and Feldheim, D. L. (2003) Multifunctional gold nanoparticle-peptide complexes for nuclear targeting. *J. Am. Chem. Soc.* **125,** 4700–4701.
4. Jin, R., Cao, Y., Mirkin, C. A., Kelly, K., Schatz, G., and Zheng, J. (2001) Photoinduced conversion of silver nanospheres to nanoprisms. *Science* **294,** 1901–1903.
5. West, J. L. and Halas, N. J. (2000) Applications of nanotechnology to biotechnology—commentary. *Curr. Opin. Biotechnol.* **11,** 215–217.
6. Grabar, K. C., Freeman, R. G., Hommer, M. B., and Natan, M. J. (1995) Preparation and characterization of Au colloid monolayers. *Anal. Chem.* **67,** 735–743.
7. Lanford, R. E., Kanda, P., and Kennedy, R. C. (1986) Induction of nuclear transport with a synthetic peptide homologous to the Sv40 T-antigen transport signal. *Cell* **46,** 575–582.
8. Hermanson, G. T. (1996) *Bioconjugate Techniques*, 1st ed., Academic, New York.
9. Hayat, M. A., ed. (1989) *Colloidal Gold: Principles, Methods, and Applications*, vol. 2, Academic, New York.
10. Demers, L. M., Mirkin, C. A., Mucic, R. C., Reynolds, R. A., Letsinger, R. L., Elghanian, R., and Viswanadham, G. (2000) A fluorescence-based method for

determining the surface coverage and hybridization efficiency of thiol-capped oligonucleotides bound to gold thin films and nanoparticles. *Anal. Chem.* **72,** 5535–5541.
11. Templeton, A. C., Wuelfing, W. P., and Murray, R. W. (2000) Monolayer-protected cluster molecules. *Acc. Chem. Res.* **33,** 27–36.
12. Xie, H., Tkachenko, A., Glomm, W., Ryan, J., Brennaman, M. K., Papanikolas, J. M., Franzen, S., and Feldheim, D. (2003) Critical flocculation concentrations, binding isotherms, and ligand exchange properties of peptide-modified gold nanoparticles studied by UV-visible, fluorescence, and time-correlated single photon counting spectroscopies. *Anal. Chem.* **75,** 5797–5805.
13. Deroe, C., Courtoy, P. J., and Baudhuin, P. (1987) A model of protein colloidal gold interactions. *J. Histochem. Cytochem.* **35,** 1191–1198.
14. Horisberger, M. and Clerc, M. F. (1985) Labeling of colloidal gold with protein A: a quantitative study. *Histochemistry* **82,** 219–223.
15. Cao, Y., Jin, R., and Mirkin, C. A. (2001) DNA-modified core-shell Ag/Au nanoparticles. *J. Am. Chem. Soc.* **123,** 7961–7962.
16. Haes, A. and Van Duyne, R. (2002) A nanoscale optical biosensor: sensitivity and selectivity of an approach based on the localized surface plasmon resonance spectroscopy af triangular silver nanoparticles. *J. Am. Chem. Soc.* **124,** 10,596–10,604.
17. Tkachenko, A. G., Xie, H., Yanli, L., Coleman, D., Ryan, J., Glomm, W., Shipton, M., Franzen, S., and Feldheim, D. L. (2004) Cellular trajectories of peptide-modified gold particle complexes: comparison of nuclear localization signals and peptide transduction domains. *Bioconj. Chem.* **15,** 482–490.
18. Inoue, S. (1981) Video image processing greatly enhances contrast, quality and speed in polarization-based microscopy. *J. Cell Biol.* **89,** 346–356.
19. Inoue, S. and Spring, K. (1997) *Video Microscopy, The Fundamentals*, 2nd ed., Plenum, New York.
20. Hoefsmit, E., Korn, C., Bliliven, N., and Ploem, J. (1986) Light microscopical detection of single 5 and 20 nm particles used for immunolabelling of plasma membrane antigens with silver enhancement and reflection contrast. *J. Microsc.* **143,** 161–169.
21. De Waele, M. (1989) Silver-enhanced colloidal gold for the detection of leucocyte cell surface antigens in dark-field and epipolarization microscopy, in *Colloidal Gold: Principles, Methods, and Applications*, vol. 2 (Hayat, M. A., ed.), Academic, New York, pp. 443–467.
22. De Brabander, M., Geerts, H., Nuyens, R., Nuydens, R., and Cornelissen, F. (1993) Nanovid microscopy: imaging and quantification of colloidal gold labels in living cells, in *Electronic Light Microscopy: Techniques in Modern Biomedical Microscopy* (Shotton, D., ed.), Wiley-Liss, New York, pp. 141–155.
23. Albrecht, M. and Hodges, G., eds. (1988) *Biotechnology and Bioapplications of Colloidal Gold*, Scanning Microscopy International, Chicago, IL.
24. Ellis, I., Bell, J., and Bancroft, J. (1989) Polarized incident light microscopical enhancement of immunogold and immunogold-silver preparations: its role in immunohistology. *J. Pathol.* **159,** 13–16.

25. De Brabander, M., Geerts, H., Nuydens, R., Geuens, S., Moeremans, M., and De Mey, J. R. (1989) Detection and use of gold probes with video-enhanced contrast light microscopy, in *Immuno-Gold Labeling in Cell Biology* (Verklej, A. J. and Leunissen, J. L. M., eds.), CRC Press, Boca Raton, FL, pp. 217–222.
26. Hunter, R. J. (2001) *Foundations of Colloid Science*, 2nd ed., Oxford University Press, Oxford, UK.
27. Udenfriend, S., Stein, S., Buhlen, P., Dairman, W., Leimgruber, W., and Weigele, M. (1972) Fluorescamine: a reagent for assay of amino acids, peptides, proteins, and primary amines in the picomole range. *Science* **178,** 871–872.